Creating and Detecting Shaped Rydberg Wave Packets

Jeffrey L. Krause,[1] Kenneth J. Schafer,[2] M. Ben-Nun,[3] and Kent R. Wilson[3]
[1]*Quantum Theory Project, P.O. Box 118435, University of Florida, Gainesville, Florida 32611-8435*
[2]*Department of Physics and Astronomy, Louisiana State University, Baton Rouge, Louisiana 70803-4001*
[3]*Department of Chemistry and Biochemistry, University of California, San Diego, La Jolla, California 92093*
(Received 8 November 1996)

Inherently quantum mechanical, transient nanostructures with dynamics on a picosecond time scale can be produced by controlling the quantum dynamics of Rydberg electrons. Ultrashort, tailored light pulses are used to build structures in position and/or momentum space from the wave function of an electron. The optimal laser pulses required to make these structures can be computed and synthesized in the laboratory. As an example, we present a structure consisting of five peaks which acts as a time-dependent grating and can be detected via ultrafast extreme ultraviolet diffraction. [S0031-9007(97)04874-6]

PACS numbers: 32.80.Rm, 31.15.–p, 32.80.Qk, 42.50.Hz

When matter is excited coherently with an ultrafast laser pulse, a nonstationary quantum superposition state, or wave packet, is created. The wave packet is composed of the eigenstates spanned by the frequency bandwidth of the laser pulse. One of the simplest experimentally realizable examples of a wave packet is the one-electron Rydberg wave packet [1]. Recent experiments have demonstrated the ability to create long-lived electronic wave packets in hydrogen and the alkali metals [2]. These wave packets can be created in the radial dimension, the angular dimension, or both [3].

Rydberg wave packets created using transform limited Gaussian pulses show a variety of semiclassical and quantum features that have made them the object of intense study over the past decade [4]. A wave packet consisting of several states around a mean excitation level $\bar{n}$ oscillates between the nucleus and the classical outer turning point $r_c = 2\bar{n}^2$ (atomic units are used throughout). If the pulse length is chosen appropriately, a minimum uncertainty packet is created on the first oscillation at r_c [1,2]. The oscillation period is set by the average energy spacing, $\tau = 2\pi\bar{n}^3$. The wave packet disperses in $\bar{n}/6$ oscillations and has a first revival after $\bar{n}/3$ oscillations. In the absence of dephasing, these revivals and fractional revivals continue long after the excitation pulse has ended [5].

One can move beyond the creation of Gaussian wave packets at the turning point of Coulomb potentials by using more complex excitation pulses. Modification of electronic wave packets using nontransform limited pulses has now been demonstrated experimentally in both atoms and semiconductors [6,7]. Since the populations and relative phases of the eigenstates that comprise the wave packet are completely determined while the laser pulse is on, the excitation process determines the future behavior of the system, even at asymptotic times. This idea forms the basis for several schemes to control the outcome of chemical reactions and other material processes [8].

In this Letter, we address two crucial issues related to the production and detection of shaped Rydberg wave packets. The first is the relationship between the complexity of the desired structure and that of the laser field that produces it. For simple targets with well separated substructures, the excitation pulse can often be viewed as consisting of independent (non-phase-locked) pulses. More complex targets require amplitude and phase modulation that can be created using various pulse-shaping technologies [9]. The second issue is the detection of tailored wave packets. Typically, the target distribution is chosen near the outer turning point of the Coulomb potential, where the electron is nearly free. Since free electrons do not absorb or emit photons, traditional pump-probe methods are sensitive only to the electronic distribution near the nucleus, and not to the distribution in the target region [2,10].

As one way of detecting controlled Rydberg wave packets we investigate the possibility of using time-dependent extreme ultraviolet (XUV) diffraction. We show that the diffraction signal provides a direct probe of the time-dependent spatial distribution of the wave packet. As an example, we discuss some of the experimental factors involved in building and detecting a five-peaked nanostructure from the wave function of a single electron. We demonstrate that this structure can be synthesized and detected with currently available laser technology. Successful completion of such experiments may lead to the ability to use lasers to control the electronic fabric of matter, and have applications in the production of nanoscale devices, communication, or chemical synthesis.

We begin by describing the construction of tailored wave packets using shaped laser pulses [11]. For illustrative purposes we concentrate on creating radial Rydberg wave packets in the hydrogen atom, with weak excitation fields. Extensions of the method to strong excitation fields, to multidimensional wave packets, and to other one-electron atoms are straightforward, and will be discussed elsewhere. In particular, the alkali metals, in which most experiments are currently performed, can be treated in our formalism by simply changing the one-electron potential. This does not alter any of the conclusions discussed below

 0031-9007/97/79(25)/4978(4)$10.00

for hydrogen. In addition, using heavier atoms aids in the detection of the shaped wave packets.

To compute the laser field for a desired packet, we use a variant of optimal control theory that has been discussed previously [12]. The idea is to choose a target operator that represents the desired outcome, and then to compute the electric field that maximizes the expectation value of the target operator, within certain constraints. In the simple cases discussed here, the target operator $\hat{A}$ is a projection operator $|\Phi_T\rangle\langle\Phi_T|$ onto a chosen distribution Φ_T in phase (position/momentum) space, at a chosen time. As noted by several authors, a variety of constraints can be imposed on the form of the optimal fields [8,12]. The effects of a given constraint on both the complexity of the optimal field and its performance must, in general, be considered carefully. In the examples presented here, the constraint is simply that the intensity of the field be nonzero and noninfinite (that is, a penalty term has been included on the spectral intensity). The form of the field is allowed to vary freely in a given time interval.

As an example of the theoretical framework, consider the wave packet depicted in Fig. 1. The target consists of a structure exhibiting five equally spaced Gaussian peaks, with separations of 36 nm. The entire structure has a small positive momentum (that is, the electron is moving away from the nucleus). The goal is to find the laser field that drives the electron from its ground state at time t_0 to maximum overlap with this target at the target time t_f. The calculation is performed for the hydrogen atom using a nonlinear, radial finite difference grid. The wave packet has angular momentum $\ell = 1$ and is composed of about 25 states with $\bar{n} \approx 45$. The globally optimal field for the target in Fig. 1 is shown in Fig. 2(a). This field produces a wave packet at the target time ($t_f - t_0 = 10$ ps) with nearly perfect overlap with the target.

The field shown in Fig. 2(a) appears, at first, to be quite complex. Some insight can be gained by considering the Wigner time-frequency distribution of the five *separate* fields needed to produce *separately* the five peaks in Fig. 1 at $t = t_f$ [Fig. 2(b)]. To do this, we use the procedure discussed above to calculate the optimal field for each peak in the target. As can be seen in the figure, the five optimal fields have slightly different center frequencies and maxima at five distinct center times. They also have considerable overlap in time/frequency space. Therefore, a laser field consisting of a sum of the five fields that produce the five peaks in Fig. 1 separately will not reproduce the five-peaked structure, unless the relative phases of the pulses can be precisely controlled. In other words, the subpulses must be phase locked. From a practical viewpoint, the field in Fig. 2(a) is best viewed as a single pulse made by amplitude and phase shaping, rather than a sum of five independent subpulses.

In certain cases, however, the optimal field can be created by summing the optimal fields for the separate substructures. For example, if the second and fourth fields are removed from Fig. 2(b), the remaining three fields have negligible overlap. This suggests that a three-peaked structure corresponding to peaks one, three, and five might be made from three separate subpulses which are not phase locked to each other. Explicit calculations verify that this is indeed the case. Note, though, that this conclusion is valid only for the rather special types of target considered in this Letter. For certain targets, phase-locked pulses are still required, even if the pulses have no temporal overlap [13]. When independent subpulses are appropriate, the

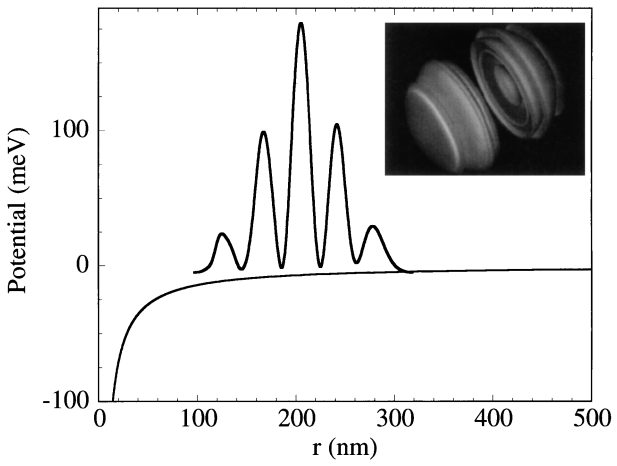

FIG. 1. Five-peaked target discussed in the text. Shown are the Coulomb potential and the wave packet density $|r\psi(r)|^2$. The inset shows the target in spherical polar coordinates.

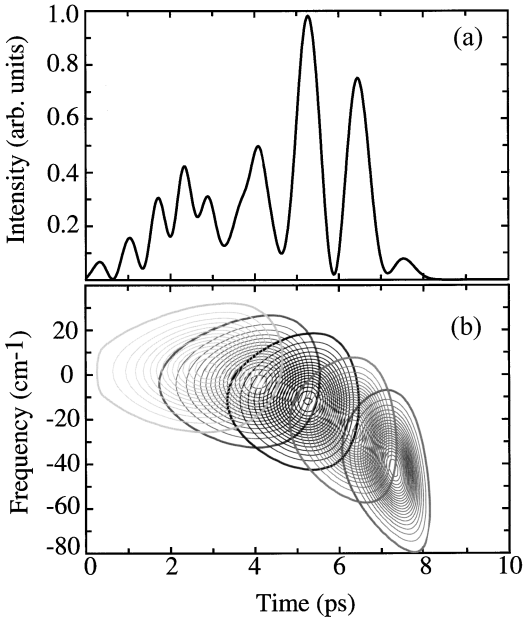

FIG. 2. Optimal field for the five-peaked target. Panel (a) shows the intensity envelope $|E(t)|^2$, and panel (b) shows a Wigner representation of the five subpulses that create separately the five peaks in the target. The wave packet produced by this field has nearly perfect overlap with the target in Fig. 1.

resulting Gaussian peaks can be thought of as a basis set that might be used to create complicated structures from much simpler building blocks [14].

Creating shaped Rydberg packets is only the first step towards demonstrating the control of electronic dynamics in atoms. Equally important is the ability to detect the shaped packets. Several possible methods have been suggested to do this, each sensitive to different properties of the wave packet. For example, pump-probe ionization of Rydberg wave packets provides information about the wave packet near the nucleus [10]. An "atomic streak camera" has been used to obtain time-resolved measurements of the ionization dynamics of Stark wave packets [15]. Wave packet interferometry can also be used to infer information about the electronic dynamics [16]. Finally, Rydberg wave packets can be probed using nearly unipolar "half-cycle" pulses [17]. The ionization signal from these pulses provides direct information about the momentum of the wave packet, that is, $|\psi(p)|^2$, rather than $|\psi(r)|^2$.

For radial targets such as those in Fig. 1, the optimal scheme for detecting the shaped wave packet is ultrafast diffraction using photons with a wavelength comparable to the nanoscale structure of the wave packet. Electron diffraction is not appropriate for these targets, because the energies required (in the meV range) are too low to be feasible experimentally. However, the photon wavelength required is in the XUV, where intense pulses are now available. If the XUV pulse is shorter than the time scale for wave packet evolution, diffraction provides a direct probe of the time-dependent, radial wave packet distribution.

In the first Born approximation, the elastic scattering cross section is proportional to the square of the atomic form factor $f(\vec{q}, t)$, which has three contributions [18],

$$f(\vec{q}, t) = N_0 f_0(\vec{q}) + N_{\mathrm{wp}} f_{\mathrm{wp}}(\vec{q}, t) + f_{\mathrm{c.t.}}. \quad (1)$$

Here, N_0 and N_{wp} are the population in the ground state and the wave packet, and f_0 and f_{wp} are the Fourier transforms of the normalized ground state and wave packet probability densities with respect to the momentum transfer $\vec{q}$. The cross term $f_{\mathrm{c.t.}}$, which results from the product of the ground state amplitude and the wave packet, oscillates on a time scale set by the excitation laser. For XUV diffraction pulses containing many optical cycles, this rapidly oscillating cross term makes no contribution to the signal [18].

For a wave packet with nanoscale structure, the optimal photon source has a wavelength on the nanometer length scale. At such wavelengths, the ground state form factor $f_0(\vec{q})$ is nearly equal to one for all $\vec{q}$ (i.e., the scattering from the ground state component is isotropic). The scattered intensity, which is proportional to $|f(\vec{q}, t)|^2$, can then be written as

$$I(\vec{q}, t) \propto N_0^2 + 2N_0 N_{\mathrm{wp}} f_{\mathrm{wp}}(\vec{q}, t) + \mathcal{O}(N_{\mathrm{wp}} f_{\mathrm{wp}})^2. \quad (2)$$

The signal oscillates about its average value with an amplitude proportional to the population of the wave packet. After subtracting the isotropic background, f_{wp} can be extracted and then inverted to give the spatial distribution of the wave packet at all times.

In Fig. 3(a) we plot $f_{\mathrm{wp}}(\theta_q)$ where $q = 2k_0 \sin(\theta_q/2)$, for the five-peaked target. We assume that $k_0 = 0.015$ a.u., which corresponds to 22.2 nm radiation. The excitation laser is polarized parallel to the z axis, the XUV pulse propagates along the y axis, θ_q is the angle in the z-y plane, and the detector is assumed parallel to the x-y plane. Note that the diffraction pattern is not cylindrically symmetric about the y axis because the wave packet has angular momentum equal to one. The diffraction pattern shows a broad enhancement at $\theta_q \approx 35°$, the angle at which the condition for constructive interference $q\Delta R = 2\pi$ is fulfilled for ΔR equal to the peak spacing. This enhancement is absent at later times, when the wave packet disperses [Fig. 3(b)]. Thus we see that the five-peaked target acts as a transient grating, diffracting light in a time-dependent manner, at a specific time, and in a specific direction.

Recording a gas phase diffraction pattern such as Fig. 3(a) requires a very bright and ultrafast pulse of photons. An appropriate light source is high harmonic generation from a nonlinear medium produced by a high repetition rate TW-class, Ti:sapphire pump laser [19]. The high harmonics from such a source are easily shorter than 100 fs [20], and a wide range of wavelengths from 8–80 nm are available. The number of scattered photons per second can be estimated as $\sigma_T \rho \ell \mathcal{F} |f|^2$, where σ_T is the Thomson cross section, ρ is the gas density, ℓ is

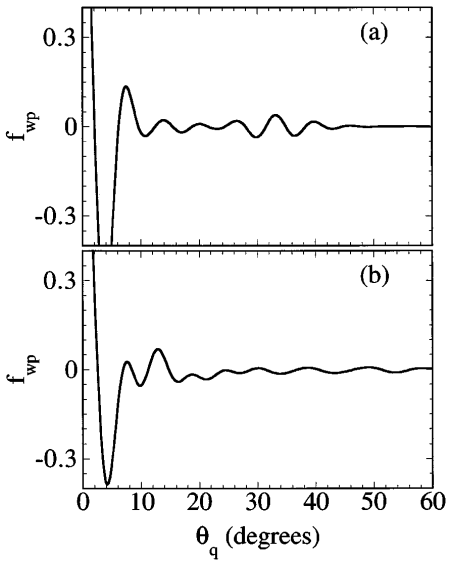

FIG. 3. XUV diffraction signal from the five-peaked target. Panel (a) shows the diffraction pattern as a function of the scattering angle at the target time, and panel (b) shows the pattern from the same wave packet one orbit (14 ps) later. The XUV wavelength is 22.2 nm.

the interaction length, and $\mathcal{F}$ is the incident photon flux. Though the cross section for electron-photon scattering is very small ($\sigma_T \sim 7 \times 10^{-24}$ cm) and there is no coherent enhancement due to periodic structure in the sample, the wave packets are aligned by the pump laser, which eliminates the need for rotational averaging. In the alkali metals, the signal is enhanced significantly, since the term N_0 in Eq. (2) is replaced by $N_0 + Z_c$, where Z_c is the number of core electrons. Thus, the total scattered signal scales as Z_c^2, and the interference term proportional to $f_{\mathrm{wp}}(\vec{q})$ scales as Z_c. Note that the background subtraction [the N_0 term in Eq. (2)] is feasible because of the vastly different length scales in the problem (a_0 versus $2\bar{n}^2 a_0$), and because the interference term depends primarily on f_{wp} and not its square.

The remaining parameters to be optimized in a realistic experimental design are the gas density ρ and the number of incident photons per second, $\mathcal{F}$. The achievable density of Rydberg atoms is controlled by several factors, including the target time and the mean excitation energy. The density scales as $\bar{n}^{-6}$, which favors targets with low $\bar{n}$. The number of high harmonic photons available depends on the energy, pulse length, and focusing characteristics of the pump laser as well as the harmonic order. Optimizing the energy and number of high harmonic photons is currently an active field of investigation, and improvements are occurring rapidly. For currently available, high-power systems, $\mathcal{F} > 10^{11}$ harmonic photons/sec may be possible, assuming a conversion efficiency of 10^{-6}. With a sample density of a few times 10^{12} atoms/cm^3 we estimate that several hundred photons/sec will be scattered by the sample, with on the order of 10 counts/sec remaining after background subtraction. The number actually observed is, of course, sensitive to the detailed experimental design. Our aim here is simply to demonstrate that the experiment is feasible, even though the scattering cross section is quite small.

In conclusion, we have shown that shaped Rydberg packets can be created and detected using experimentally feasible laser pulses and XUV diffraction. In particular, we have suggested an experiment that, while not simple, can be performed with the rapidly emerging technologies of pulse shaping and intense, high repetition rate, ultrafast lasers. Rydberg wave packets are inherently quantum systems, exhibiting quantum interference and superposition on a nearly macroscopic scale. In fact, the five-peaked structure discussed in this Letter is an example of a "Schrödinger cat" state, or a coherent superposition of (nearly) macroscopically distinct spatial states [13]. Finally, Rydberg wave packets are a natural bridge between nanotechnology and ultrafast science. They are ubiquitous in nature, allowing control schemes in such diverse systems as atoms, molecules, and semiconductors. Control of bonding in polyatomic molecules, of conductivity, or of excitonic dynamics might also be possible. Future work will include calculations of the alkali metals, multidimensional control of Stark wave packets, and a systematic exploration of the types of targets that can realistically be produced in the laboratory.

M. B. N. acknowledges the Rothschild Foundation for a postdoctoral fellowship and the United States-Israel Education Foundation for a Fulbright postdoctoral award.

[1] J. Parker and C. R. Stroud, Jr., Phys. Rev. Lett. **56**, 716 (1986).
[2] A. ten Wolde *et al.*, Phys. Rev. Lett. **61**, 2099 (1988); J. A. Yeazell *et al.*, Phys. Rev. A **40**, 5040 (1989).
[3] J. A. Yeazell and C. R. Stroud, Jr., Phys. Rev. A **35**, 2806 (1987); M. Kalinski and J. H. Eberly, Phys. Rev. Lett. **77**, 2420 (1996).
[4] G. Alber and P. Zoller, Phys. Rep. **199**, 231 (1991).
[5] J. A. Yeazell, M. Mallalieu, and C. R. Stroud, Jr., Phys. Rev. Lett. **64**, 2007 (1990).
[6] D. W. Schumacher *et al.*, Phys. Rev. A **52**, 4719 (1995).
[7] I. Broner *et al.*, J. Opt. Soc. Am. B **11**, 2457 (1994).
[8] W. S. Warren, H. Rabitz, and M. Dahleh, Science **259**, 1581 (1993); P. Brumer and M. Shapiro, Annu. Rev. Phys. Chem. **43**, 257 (1992); D. J. Tannor and S. A. Rice, Adv. Chem. Phys. **70**, 441 (1988).
[9] A. M. Weiner, J. P. Heritage, and R. N. Thurston, Opt. Lett. **11**, 153 (1986); M. Haner and W. S. Warren, Appl. Phys. Lett. **52**, 1458 (1988).
[10] L. D. Noordam *et al.*, Phys. Rev. A **40**, 6999 (1989).
[11] J. L. Krause, K. R. Wilson, and Y. J. Yan, in *Laser Techniques for State-Selected Chemistry II*, edited by J. W. Hepburn (SPIE, Bellingham, WA, 1994), p. 258.
[12] J. L. Krause *et al.*, J. Chem. Phys. **99**, 6562 (1993).
[13] M. Noel and C. R. Stroud, Jr., Phys. Rev. Lett. **75**, 1252 (1995); M. W. Noel and C. R. Stroud, Jr., Phys. Rev. Lett. **77**, 1913 (1996).
[14] B. Kohler *et al.*, Acc. Chem. Res. **28**, 133 (1995).
[15] G. M. Lankhuijzen and L. D. Noordam, Phys. Rev. Lett. **76**, 1784 (1996).
[16] R. R. Jones *et al.*, Phys. Rev. Lett. **71**, 2575 (1993).
[17] R. R. Jones, D. You, and P. H. Bucksbaum, Phys. Rev. Lett. **70**, 1236 (1993).
[18] M. Ben-Nun *et al.*, Chem. Phys. Lett. **262**, 405 (1996).
[19] J. P. Zhou *et al.*, Opt. Lett. **20**, 64 (1995); C. P. J. Barty *et al.*, Opt. Lett. **21**, 668 (1996).
[20] J. M. Schins *et al.*, J. Opt. Soc. Am. B **13**, 197 (1996).